

Ulcerative colitis and adenocarcinoma of the colon in $G\alpha_{i2}$ -deficient mice

Departments of

¹Cell Biology,

²Pharmacology;

³Pathology;

⁴Microbiology &

Immunology,

⁵Medicine,

⁶Molecular

Physiology &

Biophysics,

⁷Division of

Neuroscience,

⁸Department of

Molecular and

Human Genetics

and ⁹Howard

Hughes Medical

Institute, Baylor

College of Medicine,

One Baylor Plaza,

Houston, Texas

77030, USA

U.R. present

address: Institute of

Pharmacology,

University of

Zürich,

Winterthurerstrasse

190, CH-8057

Zürich, Switzerland

P.B. present

address: Centre

CNRS-INSERM de

Pharmacologie-

Endocrinologie, Rue

de la Cardonille,

34094 Montpellier

Cedex 2, France

G.B. and L.B.

present address:

Department of

Anesthesiology,

UCLA School of

Medicine, Center

for the Health

Sciences, 10833 Le

Conte Avenue, Los

Angeles, California

90095-1778, USA

Correspondence

should be addressed

to U.R. (Zürich) or

L.B. (Los Angeles).

Uwe Rudolph^{1,2}, Milton J. Finegold³, Susan S. Rich⁴, Gregory R. Harriman⁵,
Yogambal Srinivasan¹, Philippe Brabet¹, Guylain Boulay¹, Allan Bradley^{8,9} &
Lutz Birnbaumer^{1,5,6,7}

G proteins are involved in cellular signalling and regulate a variety of biological processes including differentiation and development. We have generated mice deficient for the G protein subunit α_{i2} ($G\alpha_{i2}$) by homologous recombination in embryonic stem cells. $G\alpha_{i2}$ -deficient mice display growth retardation and develop a lethal diffuse colitis with clinical and histopathological features closely resembling ulcerative colitis in humans, including the development of adenocarcinoma of the colon. Prior to clinical symptoms, the mice show profound alterations in thymocyte maturation and function. The study of these animals should provide important insights into the pathogenesis of ulcerative colitis as well as carcinogenesis.

G proteins are signal transducing proteins that couple a large family of receptors to effectors such as adenylyl cyclase, phospholipase C and ion channels. They often are $\alpha\beta\gamma$ heterotrimers that are referred to by their α subunits. Some 16 α -, 5 β - and 7 γ -subunit genes have been cloned so far. Although specific receptor-G protein-effector pathways have been defined for most types of G proteins¹, the true spectrum of biological functions in which they participate is still unknown.

The α -subunit of G_{i2} , α_{i2} , appears to be expressed ubiquitously and is 86–88% homologous to its close family members, α_{i1} and α_{i3} ; all three can be uncoupled from receptors by pertussis toxin (PTX). Recently, a C-terminal putatively PTX-insensitive splice variant of α_{i2} , was described which localizes to the Golgi apparatus and could be involved in membrane transport². Several specific functions have been ascribed to α_{i2} based on reconstitution experiments, stable expression of mutant forms and antisense-ablation experiments, including inhibition of adenylyl cyclase^{3–5}, stimulation of inwardly rectifying and ATP-sensitive K^+ channels^{6–8}, regulation of fibroblast proliferation⁹, stimulation of the MAP kinase pathway¹⁰, differentiation of F9 teratocarcinoma cells into primitive endoderm¹¹, and regulation of neonatal growth and development¹². Rat-1 cells transfected with the GTPase-inactivating and thus functionally activating α_{i2} mutant α_{i2} [Arg¹⁷⁹Cys] form tumours in nude mice¹³. Furthermore, GTPase-inactivating α_{i2} mutants have been found in ovarian and adrenal human tumours¹⁴ (Fig. 1a).

To learn more about the *in vivo* role of α_{i2} , we inactivated the α_{i2} gene by homologous recombination in embryonic stem cells. Remarkably, animals homozygous for this mutation develop an inflammatory bowel disease with

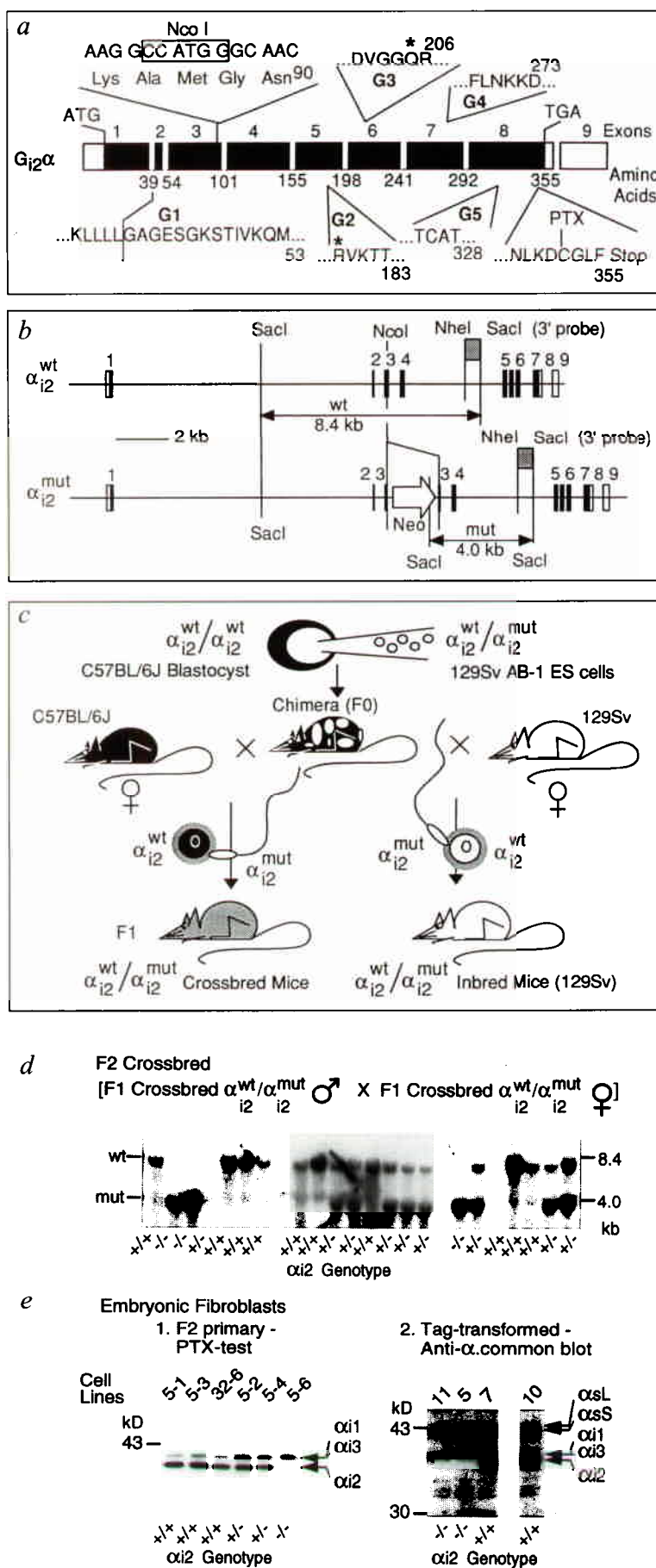
clinical and histopathological features which are strikingly similar to ulcerative colitis, including the development of adenocarcinoma of the colon.

Gene targeting and germ-line transmission

Five regions highly conserved in G-protein α subunits, G1–G5, form the pocket that binds and hydrolyses GTP¹⁵ (Fig. 1a). We disrupted α_{i2} at the *NcoI* site in exon 3 (Fig. 1b), predicting that a partial protein truncated at this point would be inactive; it would also lack the cysteine at position 352 which is ADP-ribosylated by pertussis toxin (PTX). Chimaeric mice carrying the mutant allele in their germ line¹⁶ were bred to give both crossbred (129Sv × C57BL/6J) and inbred (129Sv) α_{i2} +/– heterozygotes (Fig. 1c). Intercrosses of heterozygous animals gave rise to +/+, +/– and –/– animals (Fig. 1d). Pertussis toxin-catalyzed ADP-ribosylation of homogenates of primary fibroblasts derived from 14-day-old embryos (Fig. 1e) as well as of red blood cell membranes, and of homogenates of thymus and pancreas from 4–6-week-old animals (not shown) demonstrated the absence of mature α_{i2} protein in α_{i2} –/– animals, which was also confirmed by immunoblotting using an α -common antibody (Fig. 1e). We therefore conclude that our targeted allele is a true null allele.

Peri- and postnatal development

Analysis of the transmission of the α_{i2} –/– genotype arising from intercrossing α_{i2} +/– crossbred mice showed a mendelian distribution at embryonic day 14. However, four weeks after birth there were significantly fewer homozygous α_{i2} –/– animals (inbred or crossbred) than expected from a 1:2:1 distribution (Fig. 2a), indicating loss of homozygous mutants between these two times.



α_{i2} $-/-$ mice grow more slowly (Fig. 2*b,c*) and die prematurely (Fig. 2*d*). In contrast, α_{i2} $+/-$ animals are indistinguishable from α_{i2} $+/+$ animals for growth, life span, and pathology (see below), suggesting that the insertion of the *neo* expression cassette into the α_{i2} locus does not produce a dominant phenotype. The body weights of α_{i2} $-/-$ mice that died usually plateaued for about 2–4 weeks and then decreased over the next four weeks or so, by approximately 20–30% before death (Fig. 3*a*). α_{i2} $-/-$ mice that were losing weight had loose stools, which tested positive for occult blood (not shown).

Macroscopic and microscopic pathology

In α_{i2} $-/-$ mice, the colons had irregular dilatation and focally thickened inflamed walls of the descending portion or of the entire colon (Fig. 3*c*). In a 27-week-old mouse, perforation and localized peritonitis were found (Fig. 3*a,d*). One 36-week-old female had moderate diffuse colitis and a large mucin producing carcinoma in the cecum (Figs 3*e, 4h*). In one 41-week-old female, the duodenum was markedly dilated and congested (Fig. 3*f*). This mouse also had rectal prolapse (Fig. 3*g*). The small intestines and the other organs were otherwise unremarkable. Controls at all ages were unremarkable (example in Fig. 3*b*).

Upon microscopic examination, colitis of increasing frequency and severity was present in 21 of 26 homozygotes lacking α_{i2} . From 13 weeks onwards, every α_{i2} $-/-$ mouse had significant chronic active inflammation of the colon and every colon was most heavily inflamed distally. Initially the inflammation consisted of increased lymphocytes and plasma cells in the lamina propria and rare crypt 'abscesses' — collections of neutrophils in the lumen (Fig. 4*b*). At this stage crypt architecture and the surface epithelium were indistinguishable from normal controls (Fig. 4*a*).

Fig. 1 Targeted disruption of the α_{i2} gene. **a**, Intron–exon boundaries of the cDNA coding for α_{i2} and location of key amino acid sequences. Boxes represent exons with white representing untranslated and black representing translated sequences. Exon numbering is shown above and the number of the last amino acid of each exon is shown below the cDNA. The *NcoI* site in exon 3 that was used to disrupt the gene is shown. G1–G5; regions responsible for binding and hydrolysis of GTP. R* in G2; site of α_{i2} to *gip2* mutation found in some adrenocortical adenomas and carcinomas, and ovarian granulosa and theca cell tumours. Q* in G3; regulates GTPase activity of α_{i2} , which is reduced upon mutation to L. Pertussis toxin (PTX) ADP-ribosylates Cys at –4 from C terminus. **b**, Genomic structure of the α_{i2} gene and restriction fragment sizes for the wild-type and the mutated allele. The targeting vector IV-1 and the structure of targeted AB1-clones have been described¹⁶. A 3'-flanking probe (*NheI*–*SacI* fragment) detects a 8.4 kb fragment for the wild-type allele and a 4.0 kb fragment for the α_{i2} $-/-$ allele containing the *Neo* cassette. **c**, Clone 31A was injected into C57BL/6J blastocysts as described¹⁶. The resulting male germ-line chimaeras were bred with both C57BL/6J and 129Sv females in order to maintain the mutation in a crossbred and an inbred background, respectively. **d**, Southern blot analysis of three litters from F₁ heterozygote intercrosses showing inheritance of the α_{i2} $-/-$ genotype. **e**, Pertussis toxin-catalyzed [³²P]ADP-ribosylation of F₂ primary embryonic fibroblast homogenates and immunoblot showing absence of α_{i2} in α_{i2} $-/-$ embryos. The relative mobilities of specific G-protein α -subunits and molecular weight standards are indicated on the right and left side, respectively.

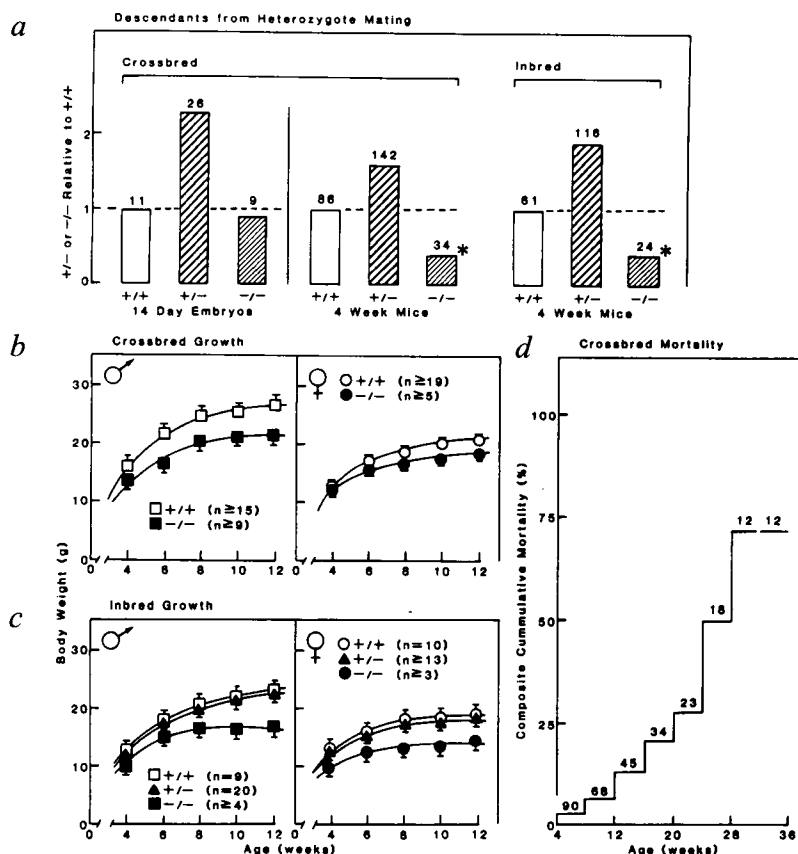


Fig. 2 Peri- and postnatal development of α_{12} -/- mice. **a**, Evidence for perinatal loss of α_{12} -/- mice. Numbers above the bars denote numbers of embryos or animals in each group. *, indicates significantly different from a mendelian 1:2:1 distribution (chi-square test with 2 degrees of freedom, 99.5% confidence). **b, c**, The progeny from crossbred (**b**) and inbred (**c**) heterozygote parents were genotyped and weighed from 4–12 weeks of age. Both male and female α_{12} -/- (-/-) mice showed a significantly decreased growth in comparison with the α_{12} +/- (+/-) and α_{12} +/+ (+/+) control mice. **d**, Cumulative mortality of α_{12} -/- crossbred mice. The cumulative mortality of α_{12} -/- crossbred mice was calculated for 4 week-periods from 4–36 weeks of age. The numbers above the line indicate the number of animals that were under observation during the respective period. There have not been enough inbred animals available to construct the equivalent mortality curve. However, the incidence of spontaneous death appears to be similar if not higher for inbred than for crossbred mice. The mean age at spontaneous death was 21.2 ± 2.1 weeks for the animals reported in (**d**) ($n=19$). By 36 weeks, 75% of the animals had died. The mean age of seven inbred α_{12} -/- mice that died spontaneously was 14.7 ± 1.8 weeks.

Ganglion cells of the myenteric plexus were normal in number, distribution and appearance at all stages. One affected male at nine weeks of age had acute ulceration of the rectum (Fig. 4c) and the distal colon was infiltrated with lymphocytes and plasma cells. In later stages neutrophils permeated and destroyed individual crypts and goblet cells were depleted of mucus. The intensity and extent of the colitis generally progressed with age. One 18-week-old female with severe colitis in the distal colon and rectum also had sharply delimited ulcers proximally without glandular mucus depletion (Fig. 4d). A nine-week-old female with mild proctitis and distal ulceration and the oldest female examined at 41 weeks, were the only mice with small intestinal inflammation (Fig. 4i).

Microscopic study of the entire viscera was performed on 12 α_{12} -/- animals (median 29 weeks) as well as on age matched controls. No significant abnormalities of other organs or tissues were found with the exception that some mice raised in our conventional facility, in which MHV and GDVII viruses were present, had evidence of acute hepatic inflammation, with numerous intralobular clusters of polymorphonuclear leukocytes. Two of the mice that died also had acute pneumonia.

Development of adenocarcinomas

α_{12} -/- mice with colonic ulcerations had foci of regenerative proliferation of glandular epithelium through the full thickness of the mucosa and in some foci both the inflammation and glandular proliferation penetrated into the submucosa (Fig. 4e). Animals with such deep inflammation had serosal inflammation as well. In six mice the presence of these regenerating glands in the submucosa suggested the possibility of invasive carcinoma,

because the epithelial cells were flat with enlarged nuclei having prominent nucleoli. Distinguishing between regenerative atypia and dysplasia was not possible. In these lesions there were no atypical mitoses or architectural features to indicate neoplasia. However, in eight mice of both sexes from 15–36 weeks of age (31% of the 26 α_{12} -/- mice examined), there were highly atypical glands showing back-to-back growth without intervening stroma, loss of nuclear polarity and severe crowding, indicating cancer of the colon (Fig. 4f). The neoplastic glands involved both mucosa and submucosa (Fig. 4g) and rarely appeared to invade the thin muscularis propria. These cancers were in all regions of the colon. Three mice had two separate cancerous foci. There were no polypoid growths. In one 36-week-female, the cecum was grossly nodular and this was due to an invasive mucin-producing carcinoma with flattened neoplastic cells surrounding the large pools of mucus in the deep submucosa and muscularis (Figs 3e, 4h). No metastatic dissemination was observed in any animal.

Immunologic functions

Flow cytometric analysis revealed a two-to-four fold increase in the proportion of α_{12} -/- thymocytes with CD4⁺8⁻ or CD4⁺8⁺ single positive phenotype characteristic of mature thymocytes (Fig. 5a). This phenotype was evident at two weeks of age and thus preceeded the inflammatory bowel disease. α_{12} -/- thymocytes also exhibited an approximately three-fold increase in cells expressing high-intensity staining of the T-cell receptor complex molecule CD3 ϵ , an additional feature of mature thymocytes. In agreement with this, 60–80% of the CD3^{hi} α_{12} -/- thymocytes expressed other cell surface markers

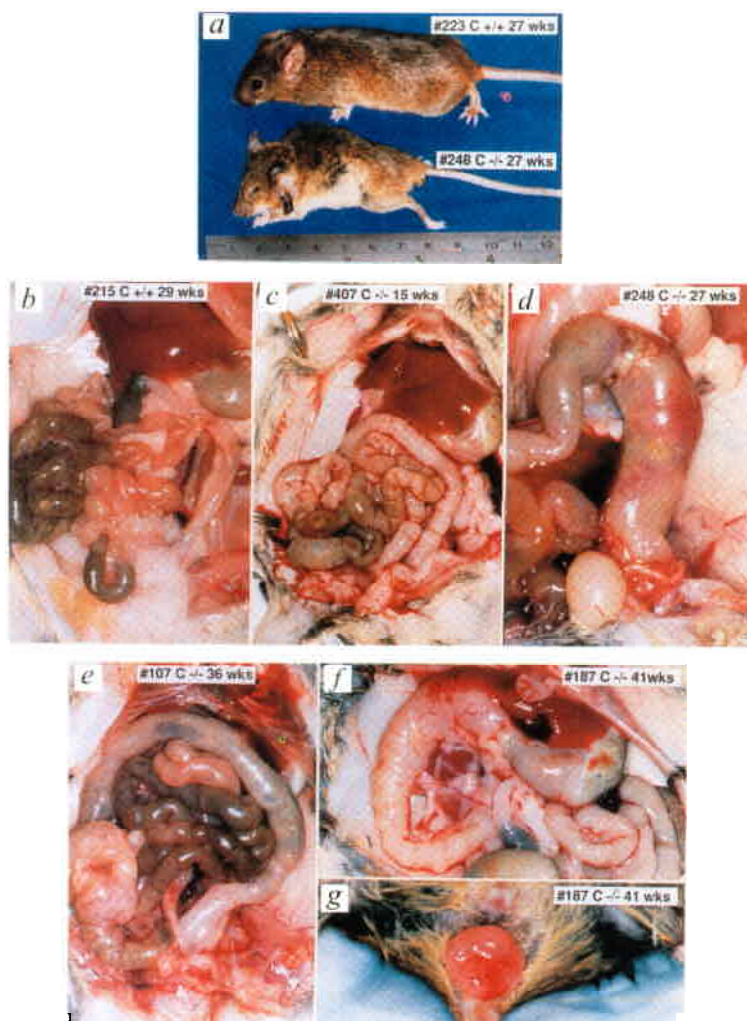


Fig. 3 Macroscopic appearance of α_2 -/- mice. Mice are identified by their number followed by C or I that indicate whether they are crossbred or inbred, genotype (+/+ , α_2 +/-; -/- , α_2 -/-) and age in weeks. *a*, 27-week-old crossbred male mice. Top, homozygous normal animal; bottom, homozygous α_2 -deficient mouse. There is marked growth retardation, weight loss, and debilitation. The affected mouse was weak with decreased muscle mass and subcutaneous fat. *B*, Abdominal viscera from 29-week-old control mouse showing the thin translucent colonic wall which collapses when empty, as in the transverse and descending colon. Fecal material can be seen through the thin wall in the sigmoid colon, cecum and ascending colon next to the hepatic flexure and the intestinal contents of the small intestine are also evident at the left. *c*, Abdominal viscera from a 18-week-old female showing mild diffuse colitis. The entire colon is slightly thickened and opaque with some congestion of the serosa. No serosal exudates are apparent. *d*, The colon of the 27-week-old α_2 -deficient mouse shown in (*a*). The descending colon is remarkably dilated and thick walled with extensive congestion and numerous serosal adhesions. In the region of the splenic flexure there is a suppurative exudate visible in the wall and a small perforation is visible at the mesenteric attachment site. The rectum of this animal had extensive inflammation and atypia of the mucosa but no carcinoma. *e*, The abdominal viscera of a 36-week-old female showing moderate diffuse colitis with extensive thickening and dilatation of the colon and rectum plus a large mass in the cecum (lower left) which proved to be a mucin secreting adenocarcinoma of the cecum (Fig. 4*h*). *f*, The upper abdominal contents of a 41-week-old female are displayed. The duodenum is remarkably thick walled and opaque compared to normal. It was diffusely inflamed along with the rest of the gastrointestinal tract. A microscopic view of the duodenum is shown in Fig. 5*i*. *g*, The anus of the 41-week-old female in (*f*) reveals rectal prolapse secondary to diffuse colitis.

found in the most mature thymocyte subset, including MEL-14^{hi}, CD44^{lo}, J11d⁻ (not shown). α_2 -/- thymocytes exhibited 3-to-5-fold higher proliferative responses to T cell receptor stimuli, including immobilized anti-CD3 ϵ antibody (with or without addition of the phorbol ester PMA), staphylococcal enterotoxin A (SEA), and BALB/c (H-2^d) T depleted splenocytes in mixed lymphocyte reactions (Fig. 5*b*, data not shown), roughly consistent with the increased frequency of mature single positive thymocytes.

In order to assess the production of cytokines that are thought to affect thymocyte development and function¹⁷, thymocytes were cultured with immobilized anti-CD3 ϵ (with or without PMA) or PMA/ionomycin. Each of these treatments stimulated α_2 -/- thymocytes to produce several-fold increased IL2, IFN γ and TNF, but not IL4 levels, even after normalization of cytokine levels to 100% CD3^{hi} cells of control and mutant populations (Fig. 5*c*, data not shown). Thus, α_2 -/- thymocytes are responsive to T cell receptor stimuli and exhibit heightened proliferation that may reflect both increased proportion of peripheral T-cell-like thymocytes and elevated cytokine levels.

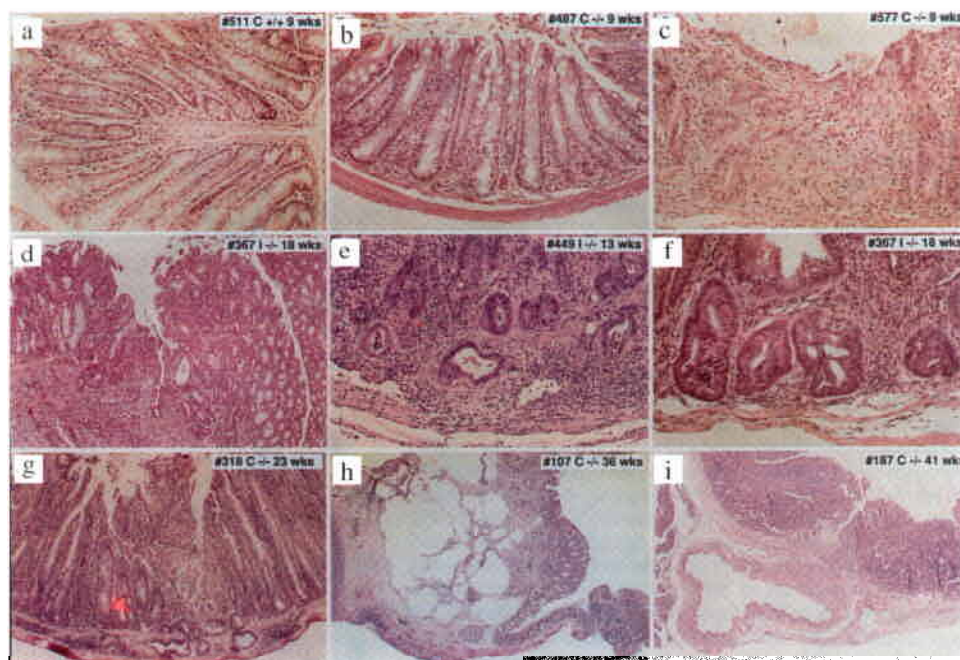
Peripheral α_2 -/- T cells in spleen and lymph node were similar to wild-type T cells in subset phenotype (Fig. 5*a*, data not shown), except for their somewhat more heterogeneous levels of CD3 expression, and

proliferative responses (Fig. 5*b*). However, α_2 -/- peripheral T cells produced IL2, IFN γ , and TNF to levels that were elevated up to 80-fold over those of wild-type T cells, depending on cytokine and stimulus. IL4 was also produced but was more modestly enhanced. (Fig. 5*c*, data not shown). Thus, α_2 -deficient mature thymocytes appear to migrate properly to spleen and lymph nodes, but retain a hyper-responsive cytokine production profile. If this over-reactive response of thymic and splenic T cells from α_2 -deficient mice also exists in mucosal T cells, it is possible that such dysfunction might contribute to the development of inflammatory bowel disease. Increased levels of IFN γ and TNF may also enhance expression of MHC class I and II antigens on cells from α_2 -deficient mice, resulting in chronically increased T cell reactivity in areas of antigen deposition.

Analysis of the B-cell phenotype in bone marrow and spleen of α_2 -deficient mice by IgM, IgD, B220 and CD23 expression did not reveal any substantial defects in development of pre-B cells, immature B cells and mature B cells. However, eight-week-old α_2 -/- mice did exhibit as much as a 20-fold increase in numbers of granulocytes in spleens and peripheral blood (data not shown).

Immunoglobulin levels were assessed in plasma and in large and small intestinal secretions¹⁸ of α_2 -/- and α_2 +/- mice. Plasma IgM levels were unaffected while plasma

Fig. 4 Histopathology of α_2 -/- mice. *a*, Colon of a nine-week-old homozygous normal female. This is a control for the subsequent pictures to show the normal histology of the colon. Glands (crypts) are lined with abundant goblet cells containing large vacuoles with mucus droplets, and are straight and regular with little intervening stroma (lamina propria) which contains only a few cells identified at higher power as lymphocytes and rare plasma cells. The border of the epithelial surface formed by the mouths of the glands, seen towards the lower left corner and along the upper part of the figure, is clearly delineated and intact. (160 \times). *b*, Nine-week-old female mouse with mild acute colitis. The crypts are slightly separated by an increase in the number of lymphocytes and plasma cells in the lamina propria. There is minimal reduction in the quantity of mucus in the goblet cells. Within the crypt in the center of the photograph, about a third from the bottom, a small cluster of neutrophils is present in the lumen (crypt abscess). (160 \times). *c*, Diffuse ulcerative colitis from the rectum of a nine-week-old female.



The surface epithelium (at the top) has been ulcerated and replaced by an inflammatory exudate. Many of the glands have been destroyed and those which remain are completely devoid of goblet cells and mucus. A high power observation showed some efforts at regeneration by the glands with mitotic activity. Most of the tissue is occupied by the chronic inflammatory infiltrate with numerous lymphocytes and plasma cells and some neutrophils (200 \times). *d*, Proximal colon of 18-week-old female showing very focal ulceration in a region which is generally well preserved and goblet cell mucus is abundant. There is mild diffuse chronic inflammation in the mucosa next to a deeply penetrating ulcer with atypical epithelium in the adjacent glands. The inflammation reaches into the submucosa. This is reminiscent of Crohn's colitis but may also represent an early adenocarcinoma. (125 \times). *e*, Rectum from a 13-week-old male. There is diffuse inflammation extending through the wall to reach the serosa. Glands are regenerating and show inflammatory atypia. (200 \times). *f*, Adenocarcinoma of colon in the same mouse shown in *d*. Back-to-back growth of highly atypical neoplastic glands without intervening stroma is seen within the submucosa. There has been attenuation of the muscularis propria. (200 \times). *g*, Adenocarcinoma of the distal colon in a 23 week old female. The photograph shows the penetration of the muscularis mucosa by atypical glands which are distorted and appear to arise from intramucosal cancer just above the muscularis mucosa. There is diffuse colitis. (125 \times) *h*, Cecal adenocarcinoma. This is the histological counterpart of Fig. 3e. An invasive mucin producing carcinoma is found within the submucosa encroaching on the muscularis propria of the cecum. (25 \times) *i*, Duodenum of the 41-week-old female illustrated in Fig. 3f. There is extensive diffuse inflammation with loss of normal villi. The inflammation extends into the submucosa to reach the common bile duct shown on left side of the picture. (50 \times)

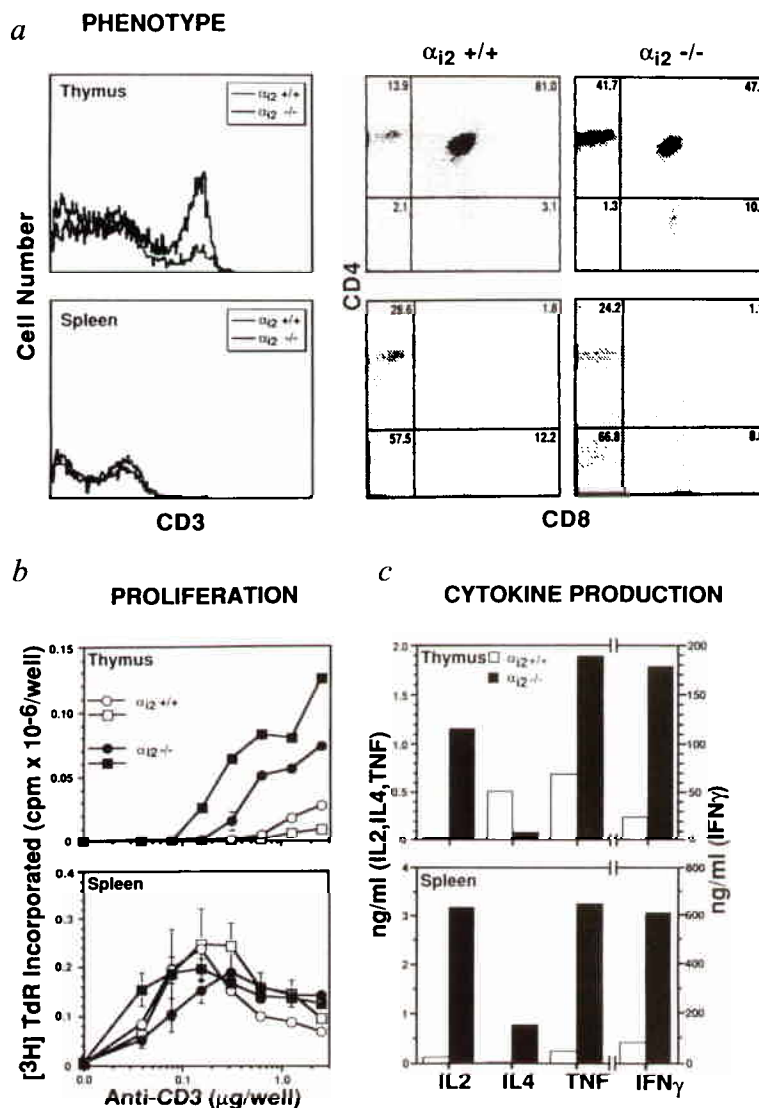
IgG and IgA levels were elevated approximately two fold in α_2 -/- mice (data not shown). Additionally, IgA in α_2 -/- mice was elevated, relative to α_2 +/+ mice, both in the small intestine [$1263 \pm 422 \mu\text{g ml}^{-1}$ (mean \pm S.D., $n=3$) versus $428 \pm 81 \mu\text{g ml}^{-1}$ (mean \pm S.D., $n=4$)] and in the large intestine [$1620 \pm 850 \mu\text{g ml}^{-1}$ versus $597 \pm 156 \mu\text{g ml}^{-1}$]. More importantly, IgG was markedly elevated in the large intestine of α_2 -/- mice ($409 \pm 58 \mu\text{g ml}^{-1}$ versus $29 \pm 17 \mu\text{g ml}^{-1}$) and more modestly in the small intestine ($106 \pm 46 \mu\text{g ml}^{-1}$ versus $26 \pm 16 \mu\text{g ml}^{-1}$). Also, IgM was elevated in the large but not the small intestine (not shown). The higher levels of IgM and especially IgG seen in the large intestine correlate with what is seen in patients with inflammatory bowel disease¹⁹. These patients have elevated numbers of IgG plasma cells in the intestine and an increase in spontaneous immunoglobulin secretion by lamina propria lymphocytes. Also, the elevated plasma levels of IgG and IgA seen in α_2 -deficient mice are similar to previous observations in patients with inflammatory bowel disease, in whom higher levels of immunoglobulin secretion by peripheral blood mononuclear cells have been found. The lower IgM and IgG levels in the small intestine of α_2 -deficient mice, as compared to large intestine, correlate with the pathological process affecting primarily the large intestine.

α_2 -/- mice free of specific pathogens

Since some mice in the colony housed in our conventional facility showed serological evidence for infection with mouse hepatitis and GDVII viruses, we assessed whether pathogens were responsible for development of disease in α_2 -/- mice. First, we surveyed an additional 15 α_2 -/- crossbred mice seronegative for viral pathogens. Seven of these animals (aged 20–51 weeks) had colitis, of which two had rectal prolapse and one had adenocarcinoma. One 36-week-old mouse presented with a normal colon but had a severely inflamed duodenum with ulcers. The remaining seronegative α_2 -/- mice (aged 17–54 weeks), were normal. Furthermore, all relevant aspects of the phenotype of α_2 -deficient mice (including weight, T-cell phenotype, inflammatory bowel disease, adenocarcinoma and spontaneous death) were also observed in seronegative mice. As the mice in the second survey belonged to generations F2–F6, whereas the mice evaluated previously belonged to generations F2 and F3, it is possible that other genetic factors can select for decreased incidence and severity of disease.

Second, we raised α_2 -deficient mice (derived by oviduct transfer of fertilized eggs) in a specific pathogen-free barrier facility. These animals also developed inflammatory bowel disease, with wasting and

Fig. 5 T-cell maturation and function in $\alpha_2(-/-)$ mice. **a**, Flow cytometric analysis of CD3, CD4 and CD8 in thymus and spleen. High intensity CD3 staining was expressed by 33.2% $\alpha_2(-/-)$ and 9.3% $\alpha_2(+/-)$ thymocytes in the example shown, while splenocytes were 34% ($\alpha_2(-/-)$) and 42.2% ($\alpha_2(+/-)$) CD3⁺. Expression of $\alpha\beta$ and $\gamma\delta$ TCR by $\alpha_2(-/-)$ thymocytes and spleen T-cells was unaffected. Twelve 8- to 12-week-old mutants were analysed with similar results. Average viable thymocyte cell yields of wild type and mutants were 96.9 and 75.2×10^6 , respectively. $\alpha_2(-/-)$ thymocyte depletion of CD4⁺8⁺ cells by *in vivo* dexamethasone and DNA fragmentation in response to *in vitro* PMA as apoptotic stimuli were indistinguishable from wild type. Splenocyte yields were 54.7 and 71.9×10^6 for $\alpha_2(+/-)$ and $\alpha_2(-/-)$. Expression of CD2, LFA-1, MEL-14, VLA-4, CD44 and CD45RB by $\alpha_2(-/-)$ and $\alpha_2(+/-)$ spleen cells were similar. **b**, Proliferative response of thymocytes and splenocytes to T-cell receptor stimulation with anti-CD3e. Mean \pm SEM [³H]TdR uptake (final 6 h culture) of triplicate cultures is shown. Responses of thymocytes and splenocytes from a given animal are identified by open (wild type) or closed (mutant) circle or square symbols. Eight $\alpha_2(-/-)$ mice have been analysed, some utilizing enriched splenic T cells, with similar results. **c**, Cytokine production by anti-CD3e activated thymocytes and spleen T cells. Cytokine concentrations (ng ml⁻¹) were normalized to 100% CD3^{hi} thymocytes or 100% CD3⁺ spleen T cells from flow cytometric quantitation of CD3 expression of each cell population. Coefficients of variance were less than 20% throughout. Data are representative of at least three independent assays.



histopathological features of colitis and adenocarcinoma of the colon, which are identical to those seen in the mice raised in the conventional facility. All 12 $\alpha_2(-/-)$ mice maintained in the barrier facility for up to 22 weeks of age were observed to develop wasting, spontaneous death and/or evidence of severe colitis and adenocarcinoma of the colon.

Discussion

We have shown that $G\alpha_{12}$ -deficient mice develop ulcerative colitis and adenocarcinoma of the colon. Mice with targeted disruption of genes for *IL2* (ref. 20), *IL10* (ref. 21) or the $\alpha\beta$ T cell receptor²² and SCID mice reconstituted with CD45RB^{hi} CD4⁺ T cells^{23,24} also develop a chronic inflammation of the bowel. However, in none of these animal models are mucosal ulcerations and colon adenocarcinoma, which are typical features in human ulcerative colitis, a characteristic feature of disease. Additional complications (such as an early lethal disease consisting of splenomegaly, lymphadenopathy, severe anaemia and, later in life, widespread amyloidosis in the *IL2*-deficient mice²¹) may also be seen in these other

models which do not appear in our α_2 -deficient mice or in humans with ulcerative colitis.

With respect to the immunological phenotype observed in our mice, there are striking similarities to transgenic mice expressing the S1 subunit of pertussis toxin from the *lck* promoter in thymocytes which functionally inactivates the $G\alpha_{12}$ and $G\alpha_{13}$ subunits. These transgenic mice also have an increased number of CD4⁺CD8⁻ and CD4⁺CD8⁺ single positive T cells with high intensity CD3 staining in the thymus but display defective lymphocyte homing in peripheral lymphoid organs^{25,26}. Whereas α_2 -deficient mice also have increased numbers of single positive (mature) T cells with high intensity CD3 staining in the thymus, they have close to normal numbers of T cells in the spleen which display unaffected proliferative responses, indicating a difference in the immunological phenotype between the two mouse strains. Our study indicates therefore that the α_2 -subunit is not essential in signalling for T-cell homing to spleen and lymph node. Very likely the homing defects induced by pertussis toxin²⁵⁻²⁷ result either from the combined loss of G_{12} and G_{13} function or just from the loss of G_{13} function. A distinction between

these two possibilities should emerge from analysis of $G\alpha_{13}$ -deficient mice. In either case, a homing defect is not likely to underly the elevated expression of mature thymocyte subsets in α_{12} -/- mice.

It is interesting to note that α_{12} is a protooncogene^{13,14,28} which apparently also has an anti-oncogenic function. Since we have not observed tumours in the absence of intestinal inflammation, we assume that the tumour formation is a consequence of the bowel inflammation with the accompanying attempts at epithelial regeneration. However, the observation that other gene-deficient mice develop inflammatory bowel disease but apparently no tumours may point to a role for α_{12} in tumour suppression. Further studies are needed to clarify the mechanisms behind these intriguing observations. Bone marrow transplantation studies are in progress to assess the relative contributions of the lymphoid compartment and the gut epithelium in the pathogenesis of disease. Of further interest is the investigation of neutrophil function, since α_{12} may play a key role in coupling receptors for chemokines such as IL-8, FMLP and leukotriene B4 to PLC- β stimulation. The increased number of neutrophils in the peripheral blood of α_{12} -deficient mice might be due their inability to migrate out of blood vessels, as is also seen in patients with leukocyte adhesion deficiency. In heart homogenates and adipocyte membranes of α_{12} -deficient mice, we observed only a partial loss of hormonal inhibition of adenylyl cyclase, indicating that receptor-G protein coupling in these mice is more selective rather than specific (manuscript in preparation).

The underlying abnormalities which lead to inflammatory bowel disease in these animals promise to shed light on the pathogenesis of ulcerative colitis in humans, as well as insight into the mechanisms of carcinogenesis. In addition, α_{12} -deficient mice will also prove valuable as a tool for the development of novel treatment strategies.

Methods

Mice. $G\alpha_{12}$ -deficient mice were generated by gene targeting (see also ref. 16). Male chimaeras were bred to both C57BL/6J and 129Sv females in order to maintain the mutation in a crossbred as well as in an inbred background. The genotype of all mice was determined by Southern blot analysis on mouse tail genomic DNA as described¹⁷. The mice were housed in microisolator cages in the open animal care facility or, where indicated, in the SPF barrier facility at Baylor College of Medicine.

[³²P]ADP-ribosylation and immunoblot analysis of fibroblast homogenates. Homogenates for [³²P]ADP-ribosylation were prepared from embryonic fibroblasts that had been derived from six embryos at embryonic day 14. Homogenization and pertussis toxin-catalyzed [³²P]ADP-ribosylation were performed as described²⁹.

Human red blood cell membranes, containing α_{11} and α_{13} , and partially purified bovine G_i/G_o, containing α_{11} , α_{12} and α_{13} , were used as markers. The pertussis toxin concentration in the reaction was 8.3 μ g ml⁻¹, the activity of the [³²P]NAD (200–400 Ci mmol⁻¹) was 4.4 \times 10⁶ cpm. The reaction was allowed to proceed for 30 min at 37 °C and stopped by the addition of 1 vol Laemmli buffer including 4 mM NAD. The whole sample was subjected to SDS-PAGE on a urea gradient (4–8 M) 9% polyacrylamide gel slab³⁰, which was then subjected to autoradiography. Membranes from T-antigen-(Tag-) transformed fibroblasts were subjected to electrophoresis and transferred onto a nitrocellulose membrane as described³¹. The membranes were probed³¹ with an anti-peptide antiserum against the common region of G protein α -subunits (α -common) (kind gift of S.M. Mumby and A.G. Gilman) recognizing, among others, the G protein subunits α_{11} , α_{12} , α_{13} , α_{14} , and α_{15} .

Histological analysis. Tissue samples were obtained in a standard fashion. Intestinal samples were usually duodenum, proximal jejunum, mid-small intestine, terminal ileum, cecum, ascending colon, mid-colon, descending colon and rectum. Samples were fixed in Bouin's solution (Sigma) or 10% buffered formalin. Specimens were embedded in paraffin and processed by the conventional hematoxylin and eosin staining method.

Analysis of T-cell maturation and function. Thymocytes, splenocytes and bone marrow cells were stained with FITC-anti-CD3e (145-2C11), PE-anti-CD4 (RM4-5), FITC anti CD8a (53-6.7), FITC anti-B220 (RA3-6B2), FITC anti-IgD α , FITC anti-CD23 (B3B4) (Pharmingen) or PE goat anti-mouse IgM (Southern Biotechnology) and analysed by single or double color analysis on an EPICS Profile (Coulter), with directly conjugated isotype controls. In order to analyze the proliferative response of thymocytes and splenocytes to T cell receptor stimulation, thymocytes (2 \times 10⁵/well) and splenocytes (4 \times 10⁵/well) from two each α_{12} -/- and α_{12} +/+ controls were cultured for 72 h in flatbottom wells with increasing concentrations of plate immobilized anti-CD3e (145-2C11) purified from ascites on protein A columns, or with staphylococcal enterotoxin A (SEA) (provided by J. Lamphear, Baylor College of Medicine) and 4 \times 10⁵/well irradiated (1500r) T cell-depleted wild-type splenocytes as antigen-presenting cells for 96 h (data not shown). For analysis of cytokine production, thymocytes and spleen T cells (4 \times 10⁵/well) were pooled from two each eight-week-old α_{12} -/- and α_{12} +/+ mice and cultured in round bottom microwells coated with anti-CD3e (2 μ g/well, thymocytes; 200 ng/well, spleen T cells) or with no stimulus or with PMA (1 ng ml⁻¹) plus ionomycin (200 ng ml⁻¹) (data not shown). At the times indicated culture supernates were harvested and quantitated by ELISA (Genzyme, Endogen) for IL2 (24 h), or for IL4, IFN γ and TNF (72 h).

Acknowledgements

We thank M. Seelig and M. Pyron for performing T-cell and B-cell analyses, respectively, T. DeMayo for embryo transfers and E. Hopkins and A. Major for preparing histological slides. U.R. and P.B. were the recipients of fellowships from the Deutsche Forschungsgemeinschaft and INSERM, respectively. This study was supported by grants from the NIH. A.B. is an Associate Investigator of the Howard Hughes Medical Institute.

Received 17 March; accepted 4 April 1995.

1. Birnbaumer, L. Receptor-to-effector signaling through G proteins: roles for $\beta\gamma$ dimers as well as for α subunits. *Cell* **71**, 1069–1072 (1992).
2. Montmayeur, J.-P. & Borrelli, E. Targeting of G_{α_2} to the Golgi by alternative spliced carboxyl-terminal region. *Science* **263**, 95–98 (1994).
3. Simonds, W. F., Goldsmith, P. K., Codina, J., Unson, C. G. & Spiegel, A. M. G_{α_2} mediates α_2 -adrenergic inhibition of adenylyl cyclase in platelet membranes: *in situ* identification with G_{α} C-terminal antibodies. *Proc. natn. Acad. Sci. U.S.A.* **86**, 7809–7813 (1989).
4. Wong, Y. H. *et al.* Mutant α subunits of G_{α_2} inhibit cyclic AMP accumulation. *Nature* **351**, 63–65 (1991).
5. Taussig, R., Iñiguez-Lluhi, J. A. & Gilman, A. G. Inhibition of adenylyl cyclase by G_{α_i} . *Science* **261**, 218–221 (1993).
6. Yatani, A., Codina, J., Sekura, R. D., Birnbaumer, L. & Brown, A. M. Reconstitution of somatostatin and muscarinic receptor mediated stimulation of K^+ channels by isolated G_{α} protein in clonal rat anterior pituitary cell membranes. *Molec. Endocrinol.* **1**, 283–289 (1987).
7. Yatani, A. *et al.* The G protein-gated atrial K^+ channel is stimulated by three distinct G_{α} -subunits. *Nature* **336**, 680–682 (1988).
8. Kirsch, G., Codina, J., Birnbaumer, L. & Brown, A. M. Coupling of ATP-sensitive K^+ channels to purinergic receptors by G-Proteins in rat ventricular myocytes. *Am. J. Physiol.* **259**, H820–H826 (1990).
9. Hermouet, S., Merendino, J. J., Gutkind, J. S. & Spiegel, A. M. Activating and inactivating mutations of the α subunit of G_{α_2} protein have opposite effects on proliferation of NIH 3T3 cells. *Proc. natn. Acad. Sci. U.S.A.* **88**, 10455–10459 (1991).
10. Gupta, S. K., Gallego, C., Johnson, G. & Heasley, L. E. MAP kinase is constitutively activated in *gip2* and *src* transformed Rat-1a fibroblasts. *J. biol. Chem.* **267**, 7987–7990 (1992).
11. Watkins, D. C., Johnson, G. L. & Malbon, C. C. Regulation of the differentiation of teratocarcinoma cells into primitive endoderm by G_{α_2} . *Science* **258**, 1373–1375 (1992).
12. Moxham, C. M., Hod, Y. & Malbon, C. C. Induction of G_{α_2} -specific antisense RNA *in vivo* inhibits neonatal growth. *Science* **260**, 991–995 (1993).
13. Pace, A. M., Wong, Y. H. & Bourne, H. R. A mutant α subunit of G_{α_2} induced neoplastic transformation of Rat-1 cells. *Proc. natn. Acad. Sci. U.S.A.* **88**, 7031–7035 (1991).
14. Lyons, J. *et al.* Two G protein oncogenes in human endocrine tumours. *Science* **249**, 655–659 (1990).
15. Noel, J. P., Hamm, H. E. & Sigler, P. B. The 2.2 Å crystal structure of transducin- α complexed with GTP γ S. *Nature* **366**, 654–663 (1994).
16. Rudolph, U., Brabet, P., Hasty, P., Bradley, A. & Birnbaumer, L. Disruption of the G_{α_2} locus in embryonic stem cells and mice: a modified hit and run strategy with detection by a PCR dependent on gap repair. *Transgenic Res.* **2**, 345–355 (1993).
17. Fischer, M. *et al.* Cytokine production by mature and immature thymocytes. *J. Immunol.* **146**, 3452–3456 (1991).
18. Elson, C. O., Ealading, W. & Lefkowitz, J. A lavage technique allowing repeated measurement of IgA antibody in mouse intestinal secretions. *J. Immunol. Meth.* **67**, 101–108 (1984).
19. Schreiber, S., Raedler, A., Stenson, W. F. & MacDermott, R. P. The role of the mucosal immune system in inflammatory bowel disease. *Gastroenterol. Clin. North Am.* **21**, 451–502 (1992).
20. Sadlack, B. *et al.* Ulcerative colitis-like disease in mice with a disrupted interleukin-2 gene. *Cell* **75**, 253–261 (1993).
21. Kühn, R., Löhler, J., Rennick, D., Rajewsky, K. & Müller, W. Interleukin-10-deficient mice develop chronic enterocolitis. *Cell* **75**, 263–274 (1993).
22. Mombaerts, P. *et al.* Spontaneous development of inflammatory bowel disease in T cell receptor mutant mice. *Cell* **75**, 275–282 (1993).
23. Morrissey, P. J., Charrier, K., Braddy, S., Liggitt, D. & Watson, J. D. CD4 $^+$ T cells that express high levels of CD45RB induce wasting disease when transferred into congenic severe combined immunodeficiency mice. Disease development is prevented by cotransfer of purified CD4 $^+$ T cells. *J. exp. Med.* **178**, 237–244 (1993).
24. Powrie, F. *et al.* Inhibition of Th1 responses prevents inflammatory bowel disease in scid mice reconstituted with CD45RB $^+$ CD4 $^+$ T cells. *Immunity* **1**, 553–562 (1994).
25. Chaffin, K. E. *et al.* Dissection of thymocyte signaling pathways by *in vivo* expression of pertussis toxin ADP-ribosyltransferase. *EMBO J.* **9**, 3821–3829 (1990).
26. Chaffin, K. E. & Perlmutter, R. M. A pertussis toxin-sensitive process controls thymocyte emigration. *Eur. J. Immunol.* **21**, 2565–2573 (1991).
27. Bargatze, R. F. & Butcher, E. C. Rapid G protein-regulated activation event involved in lymphocyte binding to high endothelial venules. *J. exp. Med.* **178**, 367–372 (1993).
28. Gupta, S. K. *et al.* Analysis of the fibroblast transformation potential of GTPase-deficient *gip2* oncogenes. *Mol. cell. Biol.* **12**, 190–197 (1992).
29. Hsu, W. H. *et al.* Molecular cloning of a novel splice variant of the α subunit of the mammalian G_{α} protein. *J. biol. Chem.* **265**, 11220–11226 (1990).
30. Codina, J., Grenet, D., Chang, K.-J. & Birnbaumer, L. Urea Gradient/SDS-PAGE: a useful tool in the investigation of signal transducing G proteins. *J. Recept. Res.* **11**, 587–601 (1991).
31. Scherer, N. M., Toro, M.-J., Entman, M. L. & Birnbaumer, L. G protein distribution in canine cardiac sarcoplasmic reticulum and sarcolemma. Comparison to rabbit skeletal membranes and brain and erythrocyte G proteins. *Arch. Biochem. Biophys.* **259**, 431–440 (1987).